Journal of Computational Applied Mechanics 2021, 52(4): 570-587
DOI: 10.22059/jcamech.2021.327163.638

RESEARCH PAPER

Analytical solution of pulsating flow and forced convection heat transfer in a pipe filled with porous medium

Fatemeh Sobhnamayan, Faramarz Sarhaddi*, Amin Behzadmehr

Department of Mechanical Engineering, University of Sistan and Baluchestan, Zahedan, Iran

Abstract

In this paper, the pulsating flow and forced convection heat transfer in a pipe filled with porous medium is investigated. The pipe is under a constant heat flux. The governing equations of the problem includes continuity, Brinkman momentum equation and energy equation. Using complex analysis technique, an analytical solution for velocity profile and temperature distribution are obtained. Also, the effect of various design parameters on velocity profile and temperature distribution is studied. Results show that the pulsating effect on velocity and temperature profile increases with the increase of Darcy number and dimensionless amplitude of pressure gradient but decreases with the increase of viscosity ratio parameter, Prandtl number and dimensionless frequency. For high dimensionless frequency ($\Omega > 30$), the maximum velocity and temperature tend to be constant due to the decrease in wave amplitude.

Keywords: Pulsating flow; Circular pipe; Porous medium; Forced convection.

1. Introduction

Considering the wide variety of mechanical movements observed in industry, it can be said that oscillating flows account for a significant part of these movements. Flow inside reciprocating pumps, internal and external combustion engines, heat exchangers, etc. are among such movements. Hence in recent years the problem of oscillating flows and its related heat transfer in pipes, channels and ducts have received considerable attention by researchers. In 1955 Womersley gave an analytical solution of the problem of viscous fluid motion in a circular tube under the periodic pressure gradient. He calculated viscous drag and flow rate. His results showed that there is a phase-lag between pressure gradient and fluid velocity [1]. In 1955 Womersley in another research gave an exact solution of the problem of viscous fluid flow in an elastic tube with thin wall, under time dependent periodic pressure gradient. It was shown that pressure wave was the cause of distortion in the tube wall and the longitudinal oscillation of it was an important factor in determining flow rate [2]. In 1961 Atabek and Chang proposed an analytical solution for unsteady oscillating flow in the entrance region of a circular tube. In order to simplify the momentum equation it was assumed that the fluid velocity in inertia terms, in the entrance region is same as the inlet velocity. They obtained the velocity profile in the entrance length versus the inlet velocity frequency [3]. In 1995 Zhao and Cheng carried out a numerical solution on convective heat transfer of reciprocating flow in a pipe with constant wall temperature. They pointed out that four dimensionless parameters of Prandtl number, kinetic Reynold number, dimensionless oscillation amplitude and length to diameter ratio govern convective heat transfer characteristic in

* Corresponding Author. Tel.: +98 54 31136465; Fax: +98 54 33447092
Email Address: fsarhaddi@eng.usb.ac.ir

reciprocating flow in pipe. They proposed a correlation in terms of kinetic Reynold number, the dimensionless oscillation amplitude and the length to diameter ratio for averaged Nusselt number [4]. In 1996 Zhao and Cheng carried out an experimental and numerical study on oscillatory laminar forced convection in a long circular tube under uniform heat flux. Their results showed that the numerical result for cycle-averaged wall temperature, centerline fluid temperature and the cycle averaged Nusselt number were in fair agreement with the obtained experimental data. They proposed a correlation for the cycle-averaged Nusselt number of a laminar oscillatory air flow in terms of appropriate similarity parameters by the experimental data [5]. In 1997 Guo and Sung obtained an improved version of Nusselt number in a laminar pulsating flow in a circular pipe by a numerical approach. Based on the obtained Nusselt number, the effect of the frequency and pulsation amplitude on heat transfer rate was investigated and it was shown that in large pulsation amplitude the most important factor that affects heat transfer enhancement is pulsation amplitude [6]. In 1997 Moschandreou and Zamir carried out an exact solution for oscillating flow in the tube with the wall of constant heat flux. They investigated the effect of pulsation frequency and Prandtl number on heat transfer. Their results showed that fluid bulk temperature and the Nusselt number were increased in the moderate range of frequency [7]. In 1997 Guo et al. carried out a numerical study on the problem of heat transfer of pulsatile flow in a circular pipe filled partially with a porous medium. In this research the effect of parameters such as thickness of porous layer, pulsating frequency, Darcy number, ratio of effective thermal conductivity of porous material to fluid and amplitude on heat transfer rate was investigated. It was shown that the increase of Darcy number causes the decrease of the dependence of effective thermal diffusivity ratio on thickness of porous layer. It was also shown that Nusselt number increases with increasing the thickness of porous layer for high conducting porous media [8]. In 2002 Habib et al. carried out an experimental research on the problem of heat transfer in laminar oscillating flow in a pipe with the wall of uniform heat flux. The effect of oscillating flow frequency and different Reynolds number on heat transfer characteristics were investigated experimentally. Their experimental data showed that the effect of oscillating flow frequency on heat transfer characteristics is more than the effect of Reynolds number [9]. In 2002 Hemida et al. investigated theoretically the effect of oscillation of laminar incompressible flow on the heat transfer in a duct with the wall of constant heat flux. In this research an exact solution of thermally fully developed region was given while for the thermal entrance length a numerical solution was carried out using finite element method. According to the solution a new coefficient in time average heat transfer equation of oscillating flow was defined. The effect of parameters such as Prandtl number, oscillating frequency amplitude and Reynold number on heat transfer rate was investigated. It was shown that oscillating flow with nonlinear thermal boundary condition (natural convection, radiation) and also turbulence caused by oscillation of flow, may result in increase of the time average Nusselt number [10]. In 2003 Sert and Beskok carried out a numerical study on convective heat transfer of oscillating flow in a channel with constant temperature at some part of top surface and uniform heat flux at the rest while the bottom surface was insulated. The obtained results were compared with the result of the corresponding one dimensional problem. The results of numerical solution included Nusselt number, time-averaged and instantaneous bulk temperature as a function of Prandtl, Womersley and penetration length. Their results showed that the steady one dimensional forced convection is more effective than the oscillating flow forced convection [11]. In 2004 Yu et al. gave an exact solution for oscillating laminar convective heat transfer in a circular tube under constant heat flux. Their results showed that Nusselt number and temperature profile fluctuate about the solution of steady laminar convection periodically. The amplitude of fluctuation is dependent on dimensionless parameters such as dimensionless oscillation frequency, dimensionless amplitude and the Prandtl number. Also, oscillation has no significant effect on time-average Nusselt number [12]. In 2006 Tsangaris et al. gave an exact solution for laminar Newtonian fluid flow in a fully developed region, driven by circumferential pressure gradient, between two concentric cylinders with porous wall. They investigated the effect of some dimensionless parameters such as Womersley number, ratio of the radii of the cylinders and transverse radial Reynolds number on flow regime, pressure and velocity profile. Their results showed that for the low values of frequency, the flow regime is quasi-steady and velocity amplitude equals nearly to the average velocity of steady flow [13]. In 2013 Yin and Ma carried out an exact solution for heat transfer in laminar oscillating flow in capillary tube with uniform heat flux as boundary condition. They used the Bessel transform technique to solve the governing equations. Based on exact solution, Nusselt number and temperature distribution were obtained. Also, they showed that Prandtle number, dimensionless oscillating amplitude and frequency are important factors affecting heat transfer of oscillating flow in capillary tubes [14]. In 2014 Yin and Ma investigated the effect of triangular pressure wave on heat transfer of oscillating flow in a circular tube. According to their results it was shown that oscillating waveform and fluid properties affect heat transfer coefficient. It was also shown that triangular waveform enhances heat transfer rate [15]. In 2016 Zallama et al. carried out a numerical study on the problem of forced convection by considering viscous dissipation in a cylinder filled with porous medium. They obtained the temperature profile and investigated the effect of different parameters such as Reynolds number, Darcy number, Eckert number, Forchheimer coefficient on temperature fields. Their results showed that the temperature increases with the increase of flow resistance in the porous region [16]. In 2016 Feldmann and Wagner carried out a direct numerical simulation on oscillatory flow in pipe for different values of dimensionless frequency and a specific shear Reynold number. They validated the results of direct numerical simulation with the related experimental data. They investigated the effect of asymmetric pressure of negative and positive half-cycle of reciprocating flow on velocity and temperature profiles. Their results showed that there is an asymmetric behavior of velocity and temperature at Womersley number of 6.5 [17]. In 2018 Jha and Yusuf carried out a numerical study on transient free convection flow between two concentric vertical cylinders. The flow was viscous and incompressible and its driving force was an internal heat generation source. The numerical data was validated by the analytical form of the steady state solution. Their results showed that the viscosity ratio is an important factor affects the impact of heat-absorbing /generating fluid [18]. In 2018 Yadav and Singh used Brinkman momentum equation to find the transient velocity profile of fully developed flow in a pipe filled with porous medium. The driving force of the flow was a constant pressure gradient (not pulsating). They used the separation of variables method to solve the governing equations, analytically. They investigated the effect of non-dimensional parameters such as Reynold number, Darcy number, Euler number and viscosity ratio on velocity profile. Their results showed that the increase of Reynold number, Darcy number and Euler number causes the increase of velocity while the viscosity ratio decreases the velocity [19]. In 2019 Brereton and Jalil investigated the temperature field of laminar fully developed flow under oscillating pressure gradient in pipes. They pointed out that there is no analytical solution for unsteady temperature field at low Womersley numbers because of non-linearity of axial temperature variation. They carried out an approximated quasi-steady analytical solution and showed that the axial conduction is main factor of the axial temperature variation [20]. In 2019 Karmakar et al. carried out a numerical analysis on forced convective heat transfer in a channel of constant heat flux and impermeable wall filled with anisotropic porous medium. They obtained the Nusselt number, temperature and velocity by considering Brinkman-Forchhimer extended Darcy model. They investigated the effect of anisotropic angle and anisotropic permeability ratio on heat transfer and hydrodynamic characteristics. Their results showed that Nusselt number varies with the anisotropic angle and ratio [21]. In 2020 Jalil studied numerically the effect of viscous heat dissipation on temperature field in oscillatory airflow in a circular tube. He proposed a correlation in terms of axial tidal displacement and Womersly number to determine dissipative bulk heating in oscillatory airflow. According to the correlation, viscous heat dissipation is important in high axial tidal displacement and Womersly number [22]. In 2020 Song and Rau investigated the hydrodynamic behavior of fluid motion inside a rotating cylindrical tank. The tank was rotating with an angular velocity which was varied from the rest state to a harmonic oscillation. They obtained an analytical solution for velocity profile in terms of dimensionless time and cylinder radius. Their results showed that dimensionless cylinder radius is an important factor to define the high velocity region near cylinder wall. In 2021 Pier and Schmid studied transient energy amplification in incompressible viscous oscillating flow in channels and pipes of constant diameter. They used a numerical method to solve the continuity, momentum and energy equation in order to obtain velocity field, flow rate and flow energy transfer. They found that at low oscillating amplitude, flow dynamics is so similar to corresponding steady flow. Their results showed that the important parameters affect transient energy amplification are, Reynolds number, Womersley numbers, perturbation wavenumbers and oscillation amplitude [24]. In 2021 Feldmann et al. investigated spatiotemporal intermittency of turbulence in pulsatile pipe flows and carried out the direct numerical simulation with two strategy. The first one, direct numerical simulation starting from a statistically steady pipe flow and the second one direct numerical simulation starting from the laminar Sexl–Womersley flow. They showed that optimal perturbation cannot maintain turbulence after the first pulsation period and, spatiotemporally intermittent turbulence maintain just for multiple periods if puffs are triggered [25]. In addition to analytical or numerical methods, the approximated-analytical methods can be used as an effective tool to solve oscillating flows [26,27].

Literature review shows that the investigation of pulsating flow and heat transfer in a pipe fully filled with porous material has not been carried out analytically. Therefore, the present research deals with this subject matter. In the present study, the problem statement and the governing equations is expressed. An analytical solution for velocity and temperature profiles is developed. Validation and parametric studies are other steps of the present study.

2. Problem Statement

The geometry and coordinate system of the problem are given in Fig. 1.

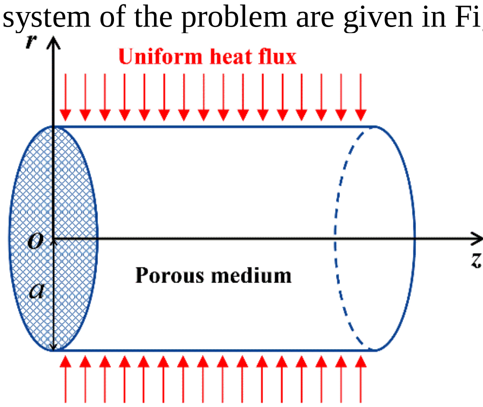

Fig. 1 Geometry of the problem

The pipe is filled with a porous medium with constant permeability. The radius of pipe is a. The outer surface of pipe is imposed to a constant uniform heat flux. The main assumptions of the problem are as follows

- Driving force of flow is an unsteady pulsating pressure gradient.
- The fluid is incompressible and Newtonian.
- Porous medium is homogeneous and isotropic.
- Thermo-physical properties of the fluid and porous medium are independent of the temperature.
- Hydrodynamically and thermally fully developed conditions are considered.

3. Governing Equations

In this section, the governing equations of pulsating flow and its related heat transfer are presented. Due to hydrodynamically fully developed flow and axial symmetry condition, the angular and radial components of fluid velocity is zero. Therefore, the fluid flow is in the direction of the pipe axis. The Brinkman momentum equation of the present problem is written as follows [19]

$$\rho\frac{\partial u}{\partial t}=-\frac{\partial P}{\partial z}+\mu_e\left(\frac{\partial^2 u}{\partial r^2}+\frac{1}{r}\frac{\partial u}{\partial r}\right)-\frac{\mu}{\kappa}u \tag{1}$$

Hydrodynamic boundary conditions of the problem are given as follows

$$\begin{aligned} &u(0,t)=\text{finite},\\ &u(a,t)=0,\\ &u(r,0)=0. \end{aligned} \tag{2}$$

The unsteady pulsating pressure gradient drives the flow in the pipe is as follows [27]

$$\frac{\partial P}{\partial z}=-A\cos(\omega t), \tag{3}$$

where u, P, A, μ_e, μ, ρ, ω, κ, a, r, z and t are axial velocity, pressure, amplitude of pressure gradient oscillations, Brinkman effective viscosity, fluid viscosity, fluid density, pulsating flow frequency, permeability, pipe radius, radial direction, axial direction and time, respectively.
The energy equation of the present problem is as follows [27]

$$\rho C_p\left(\frac{\partial T}{\partial t}+u\frac{\partial T}{\partial z}\right)=k\left(\frac{\partial^2 T}{\partial r^2}+\frac{1}{r}\frac{\partial T}{\partial r}+\frac{\partial^2 T}{\partial z^2}\right) \tag{4}$$

Thermal boundary conditions of the problem are as follows [27]

$$\begin{aligned} &T(0,z,t)=\text{finite},\\ &k\frac{\partial T(a,z,t)}{\partial r}=q'',\\ &T(r,0,t)=T_0,\\ &T(r,\infty,t)\sim z,\\ &T(r,z,0)=0. \end{aligned} \tag{5}$$

where T, T_0, q'', C_p and k are fluid temperature, inlet fluid temperature, constant heat flux on boundary, specific heat capacity, and conductivity, respectively.
The following non-dimensional quantities are introduced to obtain the non-dimensional form of the governing equations and the boundary conditions [12,14,19,27].

$$R=\frac{r}{a},\ \Omega=\frac{\omega a^2}{\nu},\ \tau=\frac{\nu t}{a^2},\ U=\frac{u}{u_m},\ u_m=a\omega,\ \ Re_\omega=\frac{2\rho u_m a}{\mu},\ M=\frac{\mu_e}{\mu},\ Da=\frac{\kappa}{a^2}, \tag{6}$$

$$\bar{A}=\frac{A}{\frac{\rho u_m \nu}{a^2}},\qquad Z=\frac{4z}{aPrRe_\omega},\qquad \theta=\frac{T-T_0}{\frac{aq''}{k}},\qquad Pr=\frac{\mu C_p}{k},\qquad Pe=Re_\omega Pr,$$

where ν, Pr, Pe, Re_ω, M and Da are kinematic viscosity, Prandtl number, Peclet number, Reynolds number, viscosity ratio parameter and Darcy number, respectively.

3.1. *Velocity Profile*

Dimensionless momentum equation and its boundary conditions are as follows

$$\begin{aligned}&\frac{\partial U}{\partial \tau}=\bar{A}\cos(\Omega\tau)+M\left(\frac{\partial^2 U}{\partial R^2}+\frac{1}{R}\frac{\partial U}{\partial R}\right)-\frac{1}{Da}U,\\&U(0,\tau)=\text{finite},\\&U(1,\tau)=0,\\&U(R,0)=0.\end{aligned}\tag{7}$$

In order to solve Eq. (7) by complex analysis technique, a complementary equation is defined as follows

$$\begin{aligned}&\frac{\partial U^*}{\partial \tau}=\bar{A}\sin(\Omega\tau)+M\left(\frac{\partial^2 U^*}{\partial R^2}+\frac{1}{R}\frac{\partial U^*}{\partial R}\right)-\frac{1}{Da}U^*,\\&U^*(0,\tau)=\text{finite},\\&U^*(1,\tau)=0,\\&U^*(R,0)=0.\end{aligned}\tag{8}$$

The summation of Eq. (7) and Eq. (8) gives an auxiliary problem of velocity profile as follows

$$\begin{aligned}&\frac{\partial \bar{U}}{\partial \tau}=\bar{A}e^{i\Omega\tau}+M\left(\frac{\partial^2 \bar{U}}{\partial R^2}+\frac{1}{R}\frac{\partial \bar{U}}{\partial R}\right)-\frac{1}{Da}\bar{U},\\&\bar{U}(0,\tau)=\text{finite},\\&\bar{U}(1,\tau)=0,\\&\bar{U}(R,0)=0.\end{aligned}\tag{9}$$

Here, the parameters $\bar{U}$ and $e^{i\Omega\tau}$ are defined as follows

$$\bar{U}(R,\tau)=U(R,\tau)+iU^*(R,\tau)\tag{10}$$

$$e^{i\Omega\tau}=\cos(\Omega\tau)+i\sin(\Omega\tau)\tag{11}$$

Due to pulsating nature of flow, the velocity profile can be considered as following [10,27]

$$\bar{U}(R,\tau)=F(R)e^{i\Omega\tau}\tag{12}$$

Substituting Eq. (12) into Eq. (9), an ordinary differential equation is obtained as follows

$$\begin{aligned}&\frac{d^2F}{dR^2}+\frac{1}{R}\frac{dF}{dR}-\eta^2F=-\frac{\bar{A}}{M},\\&F(0)=\text{finite},\\&F(1)=0.\end{aligned}\tag{13}$$

Here, the parameter η is defined as follows

$$\eta=\sqrt{\frac{1}{M}\left(\frac{1}{Da}+i\Omega\right)}\tag{14}$$

Analytical solution of Eq. (13) gives

$$F(R)=\frac{\bar{A}}{M\eta^2}\left(1-\frac{I_0(\eta R)}{I_0(\eta)}\right)\tag{15}$$

Here, $I_0(\eta R)$ is the zero order modified Bessel function of the first kind. This function can be approximated by the first three terms of its power series as follows [28]

$$I_0(\eta R) = \sum_{n=0}^{\infty} \frac{\left(\frac{1}{4}(\eta R)^2\right)^n}{(n!)^2} \approx 1 + \frac{(\eta R)^2}{4} + \frac{(\eta R)^4}{64} \tag{16}$$

Finally, the velocity profile of the problem is obtained as follows

$$U(R,\tau) = \text{Real}\left(\bar{U}(R,\tau)\right) = \text{Real}\left(\frac{\bar{A}}{M\eta^2}\left(1 - \frac{I_0(\eta R)}{I_0(\eta)}\right)e^{\mathrm{i}\Omega\tau}\right) \tag{17}$$

Here, the phrase of "Real" shows the real part of a complex number.

3.2. *Temperature Profile*

The dimensionless form of the energy equation and its boundary conditions are as follows

$$\begin{aligned} & Pr\frac{\partial\theta}{\partial\tau} + 2U\frac{\partial\theta}{\partial Z} = \frac{\partial^2\theta}{\partial R^2} + \frac{1}{R}\frac{\partial\theta}{\partial R} + \frac{16}{Pe^2}\frac{\partial^2\theta}{\partial Z^2}, \\ & \theta(0,Z,\tau) = \text{finite}, \\ & \frac{\partial\theta(1,Z,\tau)}{\partial R} = 1, \\ & \theta(R,0,\tau) = 0, \\ & \theta(R,\infty,\tau) \sim Z, \\ & \theta(R,Z,0) = 0. \end{aligned} \tag{18}$$

The complementary equation of Eq. (18) is defined as follows

$$\begin{aligned} & Pr\frac{\partial\theta^*}{\partial\tau} + 2U^*\frac{\partial\theta^*}{\partial Z} = \frac{\partial^2\theta^*}{\partial R^2} + \frac{1}{R}\frac{\partial\theta^*}{\partial R} + \frac{16}{Pe^2}\frac{\partial^2\theta^*}{\partial Z^2}, \\ & \theta^*(0,Z,\tau) = \text{finite}, \\ & \frac{\partial\theta^*(1,Z,\tau)}{\partial R} = 1, \\ & \theta^*(R,0,\tau) = 0, \\ & \theta^*(R,\infty,\tau) \sim Z, \\ & \theta^*(R,Z,0) = 0. \end{aligned} \tag{19}$$

The auxiliary problem of the temperature profile is obtained as follows

$$\begin{aligned} & Pr\frac{\partial\bar{\theta}}{\partial\tau} + 2\bar{U}\frac{\partial\bar{\theta}}{\partial Z} = \frac{\partial^2\bar{\theta}}{\partial R^2} + \frac{1}{R}\frac{\partial\bar{\theta}}{\partial R} + \frac{16}{Pe^2}\frac{\partial^2\bar{\theta}}{\partial Z^2}, \\ & \bar{\theta}(0,Z,\tau) = \text{finite}, \\ & \frac{\partial\bar{\theta}(1,Z,\tau)}{\partial R} = 1, \\ & \bar{\theta}(R,0,\tau) = 0, \\ & \bar{\theta}(R,\infty,\tau) \sim Z, \\ & \bar{\theta}(R,Z,0) = 0. \end{aligned} \tag{20}$$

Where the dimensionless temperature of $\bar{\theta}$ is defined as follows

$$\bar{\theta}(R,Z,\tau) = \theta(R,Z,\tau) + i\theta^*(R,Z,\tau) \tag{21}$$

The Eq. (20) is a partial differential equation with nonhomogeneous boundary conditions. It can be divided in to a steady and transient part as follows [10,12,14]

$$\bar{\theta}(R,Z,\tau) = \bar{\theta}_s(R,Z) + \bar{\theta}_t(R,\tau) \tag{22}$$

The equation of steady part can be obtained as follows

$$\begin{aligned} & \frac{\partial^2\bar{\theta}_s}{\partial R^2} + \frac{1}{R}\frac{\partial\bar{\theta}_s}{\partial R} + \frac{16}{Pe^2}\frac{\partial^2\bar{\theta}_s}{\partial Z^2} = 0, \\ & \bar{\theta}_s(0,Z) = \text{finite}, \end{aligned} \tag{23}$$

$$\frac{\partial \bar{\theta}_s(1,Z)}{\partial R} = 1,$$
$$\bar{\theta}_s(R,0) = 0,$$
$$\bar{\theta}_s(R,\infty) \sim Z.$$

The solution of steady temperature can be considered as follows [12,14]

$$\bar{\theta}_s(R,Z) = g(R) + f(Z). \tag{24}$$

A set of ordinary differential equations (ODEs) is obtained by substituting Eq. (24) into Eq. (23)

$$\begin{aligned} &\frac{d^2 g}{dR^2} + \frac{1}{R}\frac{dg}{dR} = -\frac{16}{Pe^2}\frac{d^2 f}{dZ^2} = C, \\ &g(0) = \text{finite}, \\ &\frac{dg(1)}{dR} = 1, \\ &f(0) = 0, \\ &f(\infty) \sim Z. \end{aligned} \tag{25}$$

The analytical solution of the above ODEs gives

$$\begin{aligned} &g(R) = \frac{R^2}{2}, \\ &f(Z) = Z. \end{aligned} \tag{26}$$

Therefore, the steady part of temperature and its derivative are as follows

$$\bar{\theta}_s(R,Z) = \frac{R^2}{2} + Z. \tag{27}$$

$$\frac{\partial \bar{\theta}_s}{\partial Z} = 1. \tag{28}$$

The equation of the transient part can be obtained as follows

$$\begin{aligned} &Pr\frac{\partial \bar{\theta}_t}{\partial \tau} + 2\bar{U}\frac{\partial \bar{\theta}_s}{\partial Z} = \frac{\partial^2 \bar{\theta}_t}{\partial R^2} + \frac{1}{R}\frac{\partial \bar{\theta}_t}{\partial R}, \\ &\bar{\theta}_t(0,\tau) = \text{finite}, \\ &\frac{\partial \bar{\theta}_t(1,\tau)}{\partial R} = 0, \\ &\bar{\theta}_t(R,0) = 0. \end{aligned} \tag{29}$$

Due to pulsating nature of the problem, the profiles of velocity and transient temperature can be written as follows [10,27]

$$\bar{U}(R,\tau) = F(R)e^{i\Omega\tau} = \frac{\bar{A}}{M\eta^2}\left(1 - \frac{I_0(\eta R)}{I_0(\eta)}\right)e^{i\Omega\tau} = \frac{\bar{A}}{M\eta^2 I_0(\eta)}\left(I_0(\eta) - 1 - \frac{\eta^2 R^2}{4} - \frac{\eta^4 R^4}{64}\right)e^{i\Omega\tau} \tag{30}$$

$$\bar{\theta}_t(R,\tau) = G(R)e^{i\Omega\tau} \tag{31}$$

Substituting Eq. (30) and Eq. (31) into Eq. (29), an ordinary differential equation is obtained as follows

$$\begin{aligned} &\frac{d^2 G}{dR^2} + \frac{1}{R}\frac{dG}{dR} - \zeta^2 G = 2F, \\ &G(0) = \text{finite}, \\ &\frac{dG(1)}{dR} = 0. \end{aligned} \tag{32}$$

Here, the parameter ζ is defined as follows

$$\zeta = \sqrt{Pri\Omega} \tag{33}$$

The analytical solution of Eq. (32) gives

$$G(R)=\frac{\bar{A}}{MI_0(\eta)}\left(-\frac{\zeta^2\eta^2+8(\zeta^2+\eta^2)}{8\zeta^5 I_1(\zeta)}I_0(\zeta R)+\frac{\eta^2R^4}{32\zeta^2}+\frac{(\zeta^2+\eta^2)R^2}{2\zeta^4}+\frac{2(\zeta^2+\eta^2)}{\zeta^6}+\frac{2(1-I_0(\eta))}{\zeta^2\eta^2}\right) \tag{34}$$

Finally, the temperature profile of the problem is obtained as follows

$$\theta(R,Z,\tau)=\text{Real}\left(\bar{\theta}(R,Z,\tau)\right)=\text{Real}\left(\bar{\theta}_s(R,Z)+\bar{\theta}_t(R,\tau)\right)=\text{Real}\left(\frac{R^2}{2}+Z+G(R)e^{i\Omega\tau}\right) \tag{35}$$

4. Validation

In the previous literature [1-29], no research was found that exactly matches the present study. However, by changing some parameters, the present problem can be adapted to other simplified cases. Yin and Ma [14] presented an analytical solution of pulsating flow and heat transfer in a pipe (without porous medium) based on Bessel transform technique. Their problem included a pulsating flow superposed on a steady flow. In the present study there is only an oscillating flow. If $M=1$ and $Da=\infty$ are chosen, the solution of the present problem can adapted with the transient part of the solution of Yin and Ma [14]. The oscillating part of velocity and temperature profiles of Yin and Ma [14] are as follows

$$U(R,\tau)=2\bar{A}\sum_{n=1}^{\infty}\frac{s_{0n}^2\cos(\Omega\tau)+\Omega\sin(\Omega\tau)}{s_{0n}J_1(s_{0n})(\Omega^2+s_{0n}^4)}J_0(s_{0n}R), \tag{36}$$

$$\bar{\theta}_t(R,\tau)=8\bar{A}\sum_{n=1}^{\infty}\left(\frac{s_{1n}(E_{2n}Pr\Omega-s_{1n}^2E_{1n})\cos(\Omega\tau)+(s_{1n}^2E_{2n}-E_{1n}Pr\Omega)\sin(\Omega\tau)}{Pr^2\Omega^2+s_{1n}^4}\right)\frac{J_0(s_{1n}R)}{J_1(s_{1n})}, \tag{37}$$

where E_{1n} and E_{2n} are defined as follows [14]

$$E_{1n}=\sum_{m=1}^{\infty}\frac{s_{0m}^2}{(\Omega^2+s_{0m}^4)(s_{0m}^2-s_{1n}^2)}, \tag{38}$$

$$E_{2n}=\sum_{m=1}^{\infty}\frac{\Omega}{(\Omega^2+s_{0m}^4)(s_{0m}^2-s_{1n}^2)}. \tag{39}$$

Here, s_0 and s_1 are the eigenvalues of the first kind Bessel function of the zero order and the first order, respectively.

Fig. 2 compares the velocity profile of the present study with the velocity profile of Yin and Ma [14] for the different values of dimensionless frequency.

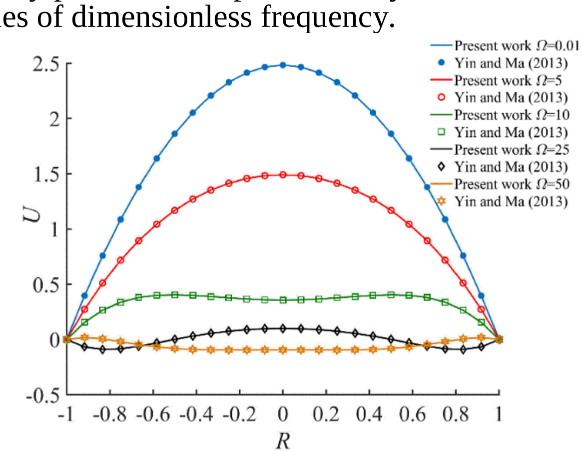

Fig. 2 Comparison of the velocity profile of the present study with the velocity profile of Yin and Ma [14] for the different values of dimensionless frequency ($\bar{A}=10,\ M=1,\ Da=\infty,\ \tau=300$).

Fig. 3 shows the transient temperature profile of the present study and Yin and Ma [14] in the different values of dimensionless frequency.

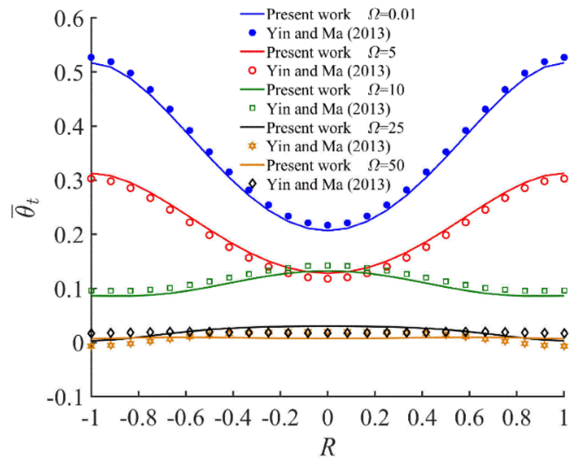

Fig. 3 Transient temperature profile of the present study and Yin and Ma [14] in the different values of dimensionless frequency ($\bar{A}=10,\ M=1,\ Da=\infty,\ Pr=1,\ \tau=300$).

According to Fig. 2 and Fig. 3, it is observed that the results of the present study for the velocity and temperature profiles are consistent with the results reported by Yin and Ma [14].

5. Parametric Studies

In this section the effect of various design parameters on the velocity and temperature profiles are studied. The constant parameters during the parametric studies are listed below of each figure. The maximum value of velocity and temperature are defined as follows [20]

$$U_{max} = |U_{avg}| = \left|\frac{1}{S}\iint U(R,\tau)dS\right|, \tag{40}$$

$$\theta_{max} = |\theta_{avg}| = \left|\frac{1}{S}\iint \theta(R,\tau)dS\right|. \tag{41}$$

The maximum value of velocity and temperature equal with the amplitude of velocity and temperature. Here, U_{avg} and θ_{avg} are the cross-sectional area averaged velocity and temperature, respectively.

5.1. Effect of Design Parameters on the Velocity Profile

Fig. 4 shows the variations of maximum velocity in terms of dimensionless frequency for different values of the Darcy number.

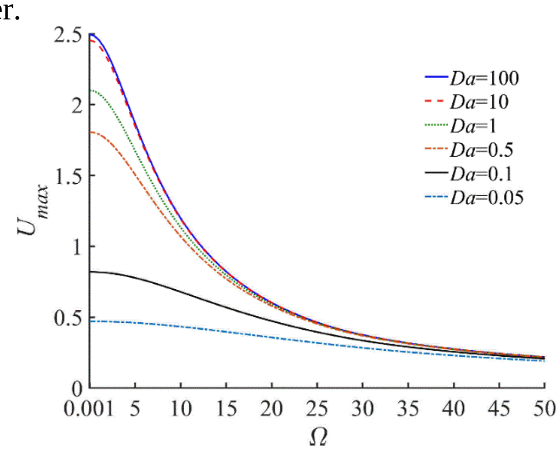

Fig. 4 Variations of maximum velocity in terms of dimensionless frequency for different values of the Darcy number ($\bar{A}=10,\ M=1$).

According to Fig. 4 it is observed that by increasing Darcy number, maximum velocity increases. The value of velocity increase in high Darcy numbers is not very high (less than 5%). Increasing Darcy number means eliminating the effect of the porous medium inside the pipe. Therefore, the frictional resistance against the flow decreases and the maximum velocity increases. On the other hands, by increasing the dimensionless frequency, the maximum velocity decreases. The increase of dimensionless frequency decreases the oscillations amplitude of velocity profile. The amplitude is the height of wave peak and the frequency is the number of oscillations in a second. Increase of frequency increases the number of oscillations in a second and decreases the height of wave peak (amplitude). Therefore, the maximum velocity decreases.

In the Fig. 5 the effect of viscosity ratio parameter on the maximum velocity for the different values of dimensionless frequency is drawn.

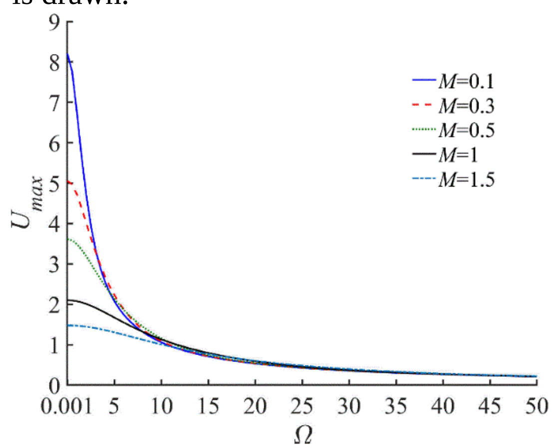

Fig. 5 Effect of viscosity ratio parameter on the maximum velocity for the different values of dimensionless frequency ($\bar{A} = 10,\ Da = 1$).

Fig. 5 shows that the maximum velocity is increased by decreasing the viscosity ratio parameter. The decrease of 70% of viscosity ratio parameter causes the increase of 60% of velocity. For the low value of the viscosity ratio parameter, the Brinkman effective viscosity is less than the fluid viscosity and the effect of the porous medium decreases. Therefore, the maximum velocity increases. According to Fig. 4 and Fig. 5, it is concluded that the increase of the Darcy number (permeability) and the decrease of the viscosity ratio parameter (Brinkman effective viscosity) enhance the velocity value.

In Fig. 6 the effect of dimensionless amplitude of pressure gradient oscillation on the maximum velocity for the different values of dimensionless frequency is shown.

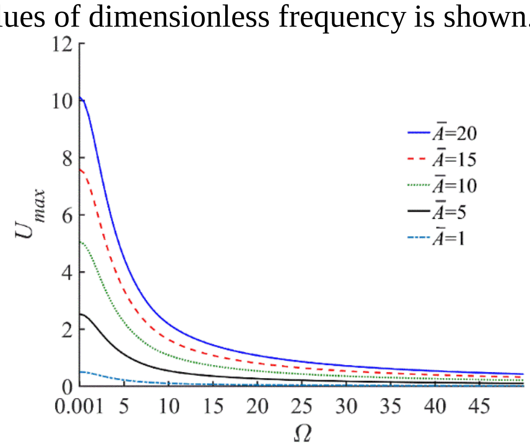

Fig. 6 Effect of dimensionless amplitude of pressure gradient oscillations on the maximum velocity for the different values of dimensionless frequency ($M = 0.3,\ Da = 1$).

According to Fig. 6, the increase of the dimensionless amplitude of pressure gradient increases the maximum velocity. The increase of velocity with the amplitude is almost linear. The pulsating pressure gradient is the driving force of the flow. It is clear that the increase of the dimensionless amplitude causes the increase of pulsating pressure gradient and consequently the increase of maximum velocity.

In order to obtain a better conception of velocity profile variations, the velocity profile for the different values of dimensionless time is plotted in Fig. 7.

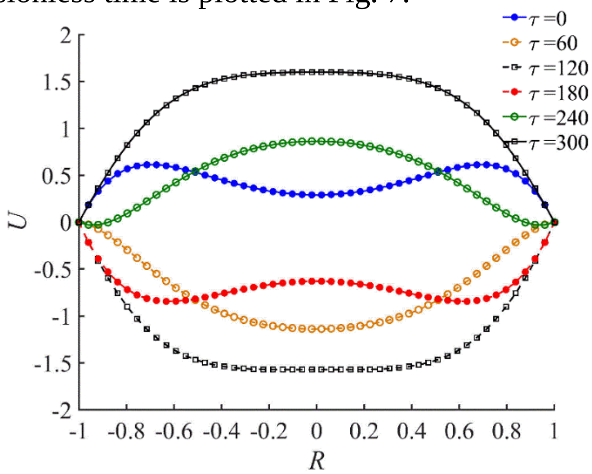

Fig. 7 Velocity profile for the different values of dimensionless time ($\bar{A} = 10,\ M = 0.3,\ Da = 1,\ \Omega = 7$).

It is seen from Fig. 7 that due to the cosine nature of pulsating pressure gradient, the change of dimensionless time causes the periodic reverse flow in the pipe. Therefore, the velocity profile also has periodical variations with respect to dimensionless time. The absolute value of velocity varies between 0 and 1.5.

5.2. Effect of Design Parameters on the Temperature Profile

The variations of maximum temperature versus the dimensionless frequency for different values of the Darcy number is shown in Fig. 8.

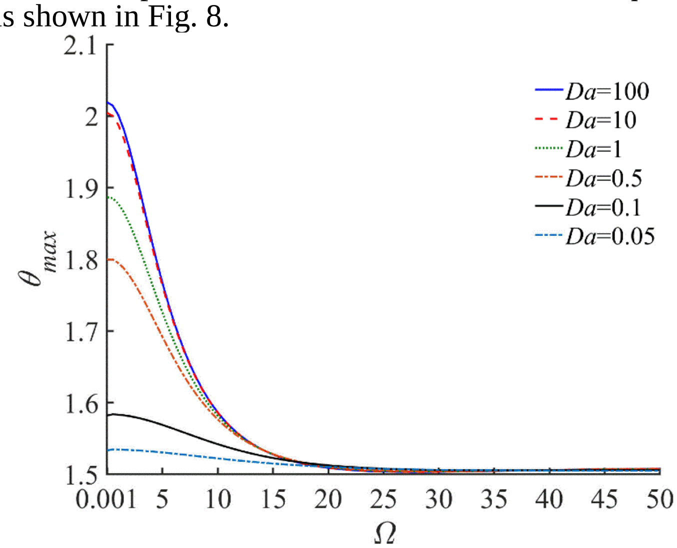

Fig. 8. Variations of maximum temperature versus the dimensionless frequency for different values of the Darcy number ($\bar{A} = 10,\ M = 1,\ Pr = 1,\ Z = 1$).

According to Fig. 8, by increasing Darcy number the maximum temperature increases. The increase of Darcy number decreases the effect of porous medium on flow velocity inside the pipe. The decrease of permeability increases the flow velocity. Therefore, the maximum fluid temperature increases by advection process. On the other hand, the increase of dimensionless frequency decreases the oscillations amplitude of temperature profile and the maximum temperature.

Fig. 9 shows the effect of viscosity ratio parameter on the maximum temperature for the different values of dimensionless frequency.

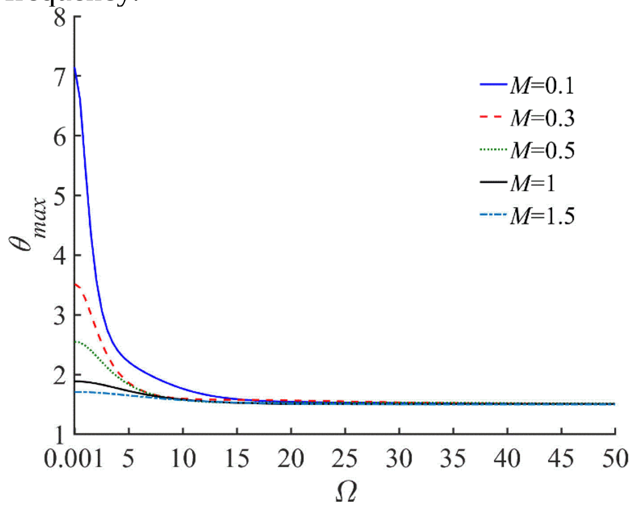

Fig. 9 Effect of viscosity ratio parameter on the maximum temperature for the different values of dimensionless frequency ($\bar{A} = 10,\ Da = 1,\ Pr = 1,\ Z = 1$).

As can be observed from Fig. 9, the increase of viscosity ratio parameter decreases the maximum temperature. Changes in viscosity ratio from 0.1 to 1.5 lead to a change in temperature from 7 to 1.7. The increase of viscosity ratio parameter means the increase of the Brinkman effective viscosity. Therefore, the fluid shear stress increases and consequently the velocity and temperature decrease.

Fig. 10 presents the effect of dimensionless amplitude of pressure gradient oscillations on the maximum temperature for the different values of dimensionless frequency.

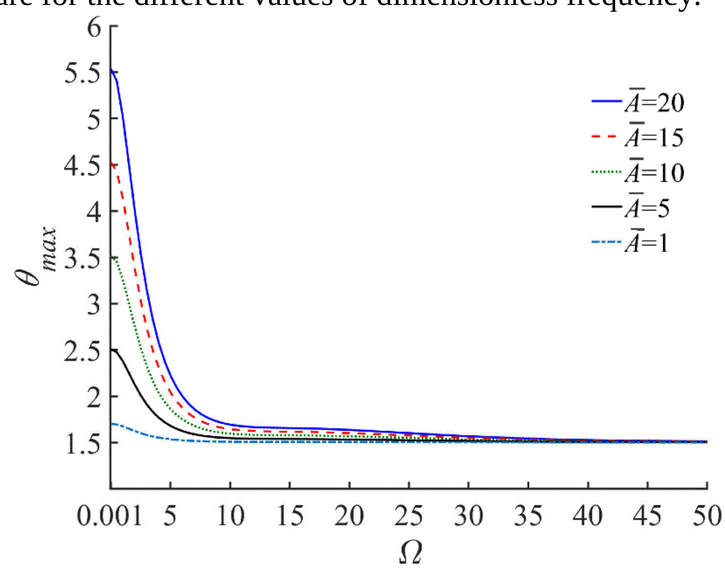

Fig. 10 Effect of dimensionless amplitude of pressure gradient oscillations on the maximum temperature for the different values of dimensionless frequency ($M = 0.3,\ Da = 1,\ Pr = 1,\ Z = 1$).

According to Fig. 10, increasing the amplitude of pressure gradient oscillations increases the maximum temperature. This increase is almost linear. The driving force of flow is the pulsating pressure gradient. The increase of amplitude of pressure gradient increases the flow velocity and the increase of flow velocity increases the maximum temperature by advection process.

In Fig. 11, the effect of Prandtl number on the maximum temperature for the different values of dimensionless frequency is depicted.

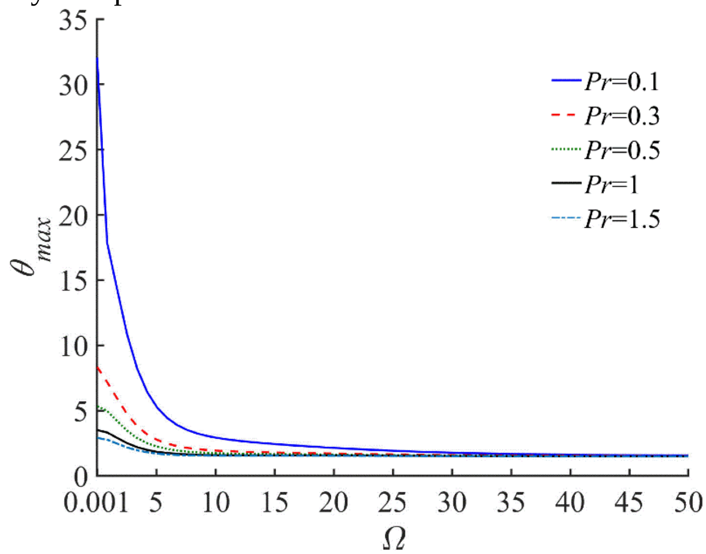

Fig. 11 Effect of Prandtl number on the maximum temperature for the different values of dimensionless frequency ($\bar{A} = 10,\ M = 0.3,\ Da = 1,\ Z = 1$).

It is observed from Fig. 11 that with the increase of Prandtl number, the maximum temperature decreases. The Prandtl number is defined as the ratio of momentum diffusivity to thermal diffusivity. For small values of Prandtl number $(Pr < 1)$, thermal diffusivity dominates over momentum diffusivity. Therefore, the maximum temperature is higher in low Prandtl numbers.

Fig. 12 shows the variations of the maximum temperature with respect to the dimensionless pipe length.

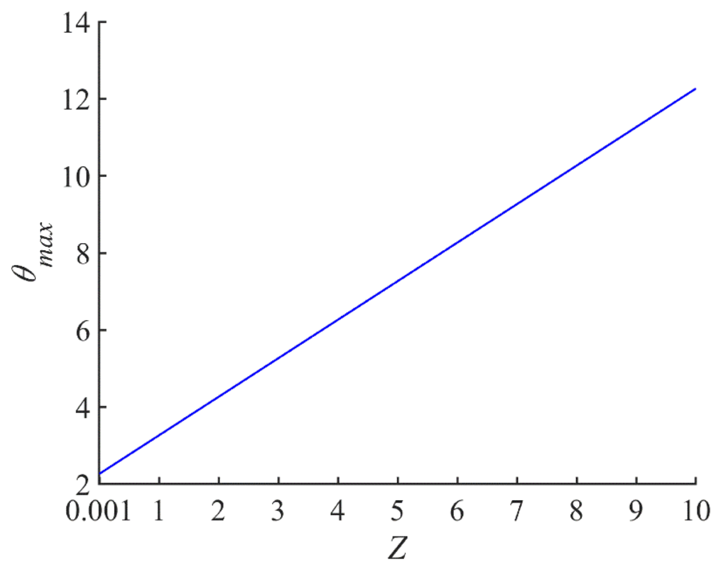

Fig. 12 Variations of the maximum temperature with respect to the dimensionless pipe length ($\bar{A} = 10,\ M = 0.3,\ Da = 1,\ \Omega = 7,\ Pr = 1$).

Considering Fig. 12, it is observed that the maximum temperature increases linearly by increasing the dimensionless length of pipe. It is a common knowledge in convection heat transfer that the temperature slope is constant for flow inside the pipe under uniform heat flux. The results of Fig. 12 also follow this fact. There is a reverse axial conduction in a pipe under uniform heat flux. This inverse axial conduction prevents the exponential growth of temperature. Therefore, the temperature variation is linear.

In order to more comprehensive study, a sample of temperature profiles is given in Fig. 13.

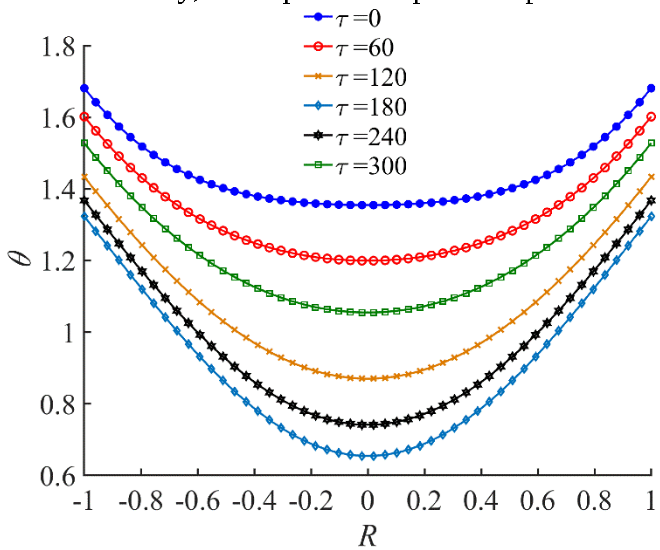

Fig. 13 Temperature profile for the different values of dimensionless time ($\bar{A} = 10,\ M = 0.3,\ Da = 1,\ \Omega = 7,\ Pr = 1,\ Z = 1$).

It is observed from Fig. 13 that the temperature decreases from the pipe wall to the pipe center. Its reason is clear. The pipe wall is subject to a constant heat flux. The fluid near the wall is definitely hotter than the fluid in the center of the pipe. On the other hands, due to the periodical nature of the flow, the temperature also has periodical variations with respect to dimensionless time.

6. Conclusion

In the present study using the complex analysis the hydrodynamic and thermal governing equations of a pulsating flow in a pipe filled with porous medium is solved analytically. The concluding remarks of the present study are as follows

- The analytical results of the present study obtained by the complex analysis technique are consistent with other analytical techniques such as the Bessel transform technique.
- The pulsating effect on maximum velocity and temperature increases with the increase of Da and $\bar{A}$ while decreases with the increase of M, Pr and Ω.
- Due to the presence of reverse axial conduction, the temperature variations with respect to dimensionless axial length is linear.
- For high frequency values, the maximum velocity and temperature tend to be constant due to the decrease in wave amplitude.

Nomenclature

a	radius of pipe (m)
A	amplitude of pressure gradient oscillations (Pa/m)
$\bar{A}$	dimensionless amplitude of pressure gradient oscillations
C	constant of separation

C_p	specific heat capacity (J/kg.^{o}C)
Da	Darcy number
E_1	constant defined by Eq. (38)
E_2	constant defined by Eq. (39)
f	function defined by Eq. (26)
F	function defined by Eq. (15)
g	function defined by Eq. (26)
G	function defined by Eq. (34)
i	unit imaginary number
I_0	zero order modified Bessel function of the first kind
J_0	zero order Bessel function of the first kind
J_1	first order Bessel function of the first kind
k	thermal conductivity (W/m.^{o}C)
M	viscosity ratio parameter
P	pressure (Pa)
Pe	Peclet number
Pr	Prandtl number
q''	constant heat flux (W/m^2)
r	radial direction
R	dimensionless radial direction
Re_ω	Reynolds number
Real	real part of a complex number
s_0	eigenvalues of the first kind Bessel function of the zero order
s_1	eigenvalues of the first kind Bessel function of the first order
t	time (s)
T	temperature (^{o}C)
T_0	inlet temperature (^{o}C)
u	velocity (m/s)
u_m	reference velocity (m/s)
U	dimensionless velocity
U_{max}	dimensionless maximum velocity
$\bar{U}$	dimensionless velocity in auxiliary problem
U^*	dimensionless velocity in complementary problem
z	axial direction
Z	dimensionless axial direction
Greek symbols	
ζ	constant defined by Eq. (33)
η	constant defined by Eq. (14)
θ	dimensionless temperature
θ_{max}	dimensionless maximum temperature
$\bar{\theta}$	dimensionless temperature in auxiliary problem
θ^*	dimensionless temperature in complementary problem
$\bar{\theta}_t$	transient part of dimensionless temperature
$\bar{\theta}_s$	steady part of dimensionless temperature
κ	permeability (m^2)
μ	fluid viscosity (N.s/ m^2)
μ_e	Brinkman effective viscosity (N.s/m^2)

ν kinematic viscosity (m^2/s)
ρ fluid density (kg/m^3)
τ dimensionless time
ω pulsating flow frequency (Hz)
Ω dimensionless pulsating flow frequency

References

[1] Womersley J.R., 1955, Method for the calculation of velocity, rate of flow and viscous drag in arteries when the pressure gradient is known, The Journal of physiology 127(3): 553-563.

[2] Womersley J.R., 1955, Oscillatory motion of a viscous liquid in a thin-walled elastic tube-I: The linear approximation for long waves, Philosophical Magazine 46(373): 199-221.

[3] Atabek H.B., Chang C.C., 1961, Oscillatory flow near the entry of a circular tube, Zeitschrift für angewandte Mathematik und Physik ZAMP 12(3): 185-201.

[4] Zhao T., Cheng P., 1995, A numerical solution of laminar forced convection in a heated pipe subjected to a reciprocating flow, International Journal of Heat and Mass Transfer 38(16): 3011-3022.

[5] Zhao T.S., Cheng P., 1996, Oscillatory heat transfer in a pipe subjected to a laminar reciprocating flow, Journal of Heat Transfer, 118(3): 592-597.

[6] Guo Z., Sung H.J., 1997, Analysis of the Nusselt number in pulsating pipe flow, International Journal of Heat and Mass Transfer 40(10): 2486-2489.

[7] Moschandreou T., Zamir M., 1997, Heat transfer in a tube with pulsating flow and constant heat flux, International Journal of Heat and Mass Transfer 40(10): 2461-2466.

[8] Guo Z., Kim S.Y., Sung H.J., 1997, Pulsating flow and heat transfer in a pipe partially filled with a porous medium, International Journal of Heat and Mass Transfer 40(17): 4209-4218.

[9] Habib M.A., Attya A.M., Eid A.I., Aly A.Z., 2002, Convective heat transfer characteristics of laminar pulsating pipe air flow, Heat and Mass Transfer 38(3): 221-232.

[10] Hemida H.N., Sabry M.N., Abdel-Rahim A., Mansour H., 2002, Theoretical analysis of heat transfer in laminar pulsating flow, International Journal of Heat and Mass Transfer 45(8): 1767-1780.

[11] Sert C., Beskok A., 2003, Numerical simulation of reciprocating flow forced convection in two-dimensional channels, Journal of Heat Transfer 125(3): 403-412.

[12] Yu J.C., Li Z.X., Zhao. T.S, 2004, An analytical study of pulsating laminar heat convection in a circular tube with constant heat flux, International Journal of Heat and Mass Transfer 47(24): 5297-5301.

[13] Tsangaris S., Kondaxakis D., Vlachakis N.W., 2006, Exact solution of the Navier–Stokes equations for the pulsating Dean flow in a channel with porous walls, International Journal of Engineering Science 44(20): 1498-1509.

[14] Yin D., Ma H.B., 2013, Analytical solution of oscillating flow in a capillary tube, International Journal of Heat and Mass Transfer 66: 699-705.

[15] Yin D., Ma H.B., 2014, Analytical solution of heat transfer of oscillating flow at a triangular pressure waveform, International Journal of Heat and Mass Transfer 70: 46-53.

[16] Zallama B., Zili Ghedira L., Nasrallah S.B., 2016, Forced convection in a cylinder filled with porous medium, including viscous dissipation effects, Journal of Applied Fluid Mechanics 9(1): 139-145.

[17] Feldmann D., Wagner C., 2016, On phase asymmetries in oscillatory pipe flow, Notes on Numerical Fluid Mechanics and Multidisciplinary Design, 132:113-122.

[18] Jha B.K., Yusuf T.S, 2018, Transient-free convective flow with heat generation/absorption in an annular porous medium: a semi-analytical approach, Proceedings of the Institution of Mechanical Engineers, Part E: Journal of Process Mechanical Engineering 232(5): 599-612.

[19] Yadav S.L., Singh A.K., 2018, Transient flow in a circular cylinder filled with porous material, International Journal of Applied and Computational Mathematics 4(6): 1-13.

[20] Brereton G.J., Jalil S.M., 2019, Axial conduction and dissipation in oscillatory laminar pipe flow at low and high frequencies, Physics of Fluids 31(8): 083607.

[21] Karmakar T., Reza M., Raja Sekhar G.P., 2019, Forced convection in a fluid saturated anisotropic porous channel with isoflux boundaries, Physics of Fluids 31(11): 117109.

[22] Jalil S.M., 2020, Numerical characterization of viscous heat dissipation rate in oscillatory air flow, Journal of Heat Transfer 142(1): 011801.

[23] Song Y., Rau M.J., 2020, Viscous fluid flow inside an oscillating cylinder and its extension to Stokes' second problem, Physics of Fluids 32(4): 043601.

[24] Pier B., Schmid P.J., 2021, Optimal energy growth in pulsatile channel and pipe flows, HAL Archives-Ouvertes, HAL Id: hal-03084366v2, https://hal.archives-ouvertes.fr/hal-03084366v2, Accessed 12 July 2021.

[25] Feldmann D., Morón D., Avila M., 2021, Spatiotemporal intermittency in pulsatile pipe flow, Entropy 23(1): 46.

[26] Deghmoum M., Ghezal A., Abboudi S., 2015, Analytical and numerical study of a pulsatile flow in presence of a magnetic field, International Journal of Physical Sciences 10(24): 590-603.

[27] Mahian O., Mahmud S., Pop I., 2012, Analysis of first and second laws of thermodynamics between two isothermal cylinders with relative rotation in the presence of MHD flow, International Journal of Heat and Mass Transfer 55: 4808-4816.

[28] Hooman K., Gurgenci H., 2007, A theoretical analysis of forced convection in a porous-saturated circular tube: Brinkman–Forchheimer model, Transport in Porous Media 69(3): 289-300.

[29] Rauf A., 2019, An analytical and semi-analytical study of the oscillating flow of generalized Burgers' fluid through a circular porous medium, Journal of Applied and Computational Mechanics 5(5): 827-839.